The Study of Visual Image Improvement of an Organic Light-Emitting Diode by Dye-Polarizer Composed of Optical Film

Wen Jeng Lan and Ho Shing Wu
Dept. of Chemical Engineering and Materials Science, Yuan Ze University, Taoyuan 32003, Taiwan

DOI 10.1002/aic.12709
Published online July 13, 2011 in Wiley Online Library (wileyonlinelibrary.com).

The visual image improvement of an organic light-emitting diode (OLED), which is based on some theoretical frameworks and the optical property of the dye-polarizer composed of optical film, is investigated. The key performance indexes of visions, i.e., visual reflective sensitivity, contrast ratio, and color saturation are focused. First, the reflectance and color saturation of an OLED were simulated and calculated by using the transfer matrix method with thin-film optical filters and the definition rule of color performances in the 1931 index proposed by the Commission International de l'Eclairage (CIE_{1931}). The results clearly showed excellent performance when using the dye-polarizer on the panel of an OLED in the theoretical calculation and practical application. © 2011 American Institute of Chemical Engineers AIChE J, 58: 1755–1763, 2012
Keywords: organic light-emitting diode, visual reflective sensitivity, contrast ratio, color saturation

Introduction

When industry innovations change as quickly as they are created, our vision and actions are influenced by the abundance of innovations in the information technology era. In the past, the cathode ray tube (CRT) techniques were developed to the point of maturity and were superior in many ways. Because of size and power consumption, CRTs have been replaced by flat panel displays (FPDs). New generation displays are required to process sufficient information content and operate in various applications. Such displays include liquid crystal displays (LCDs), plasma display panels, field emission displays, and organic light-emitting diodes (OLEDs). All these types of displays offer excellent performance and conform to the aforementioned requirements of new generation FPDs. Among these candidates, OLEDs have attracted considerable attention because of their many advantages, such as self-emission, simple structure, high response time, and wide viewing angle. OLEDs have already been used in commercial applications, such as small screens for mobile phones and portable digital audio players, car radios, digital cameras, and so on.[1–3] Moreover, OLEDs are recognized to have the greatest potential to become the next generation of display devices[4] and planar lighting source.[5,6]

Kodak developed the first efficient organic light-emitting device, and the functional performance of multilayer OLEDs was demonstrated by Tang and Vanslyke in 1987.[7] OLEDs have also received a great deal of attention due to many of their advantages in the recent years. The multilayer architecture of OLED is combined in something like a sandwich, which includes the hole injection layer (HIL), hole transporting layer (HTL), emitting material layer (EML), electron transporting layer (ETL), and electron injection layer (EIL), respectively. The multilayer architecture is between the transparent hole injecting anode and the electron injecting cathode metal. Thus, the organic emitting layers can be chosen by the adaptive dopant, codopant, and/or cohost mechanisms.[8–10]

The cathode metals of OLEDs lead to vigorous reflection in strong ambient light and the decrease in visual sensitivity, contrast ratio (CR), color saturation, and view angle chromatism of the screen image. In the past, the portable applications favored the high light output of OLEDs for readability in strong ambient light. Therefore, they have been applied to OLEDs for the methods of improving the out-coupling light efficiency. For example, the emission of light and external coupling in OLEDs has been investigated and the thickness of the indium tin oxide (ITO) layer has been controlled to reduce the energy loss in the high-index layer.[11] A pyramidal array light-enhancing layer on an OLED panel has been optimized experimentally to enhance the luminance efficiency with a gain factor of 2.03.[12] Furthermore, if increasing the high light emission to compensate for reflection, it will lead to the short lifetime of the product and human eye strain. Improving the CR of the panels could provide a solution to promote readability. A high-contrast OLED was fabricated using a gradient refractive index anode to reduce reflectance of the ambient light of the device.[13] Furthermore, various studies have used the optical interference effect to develop multilayer architectures black electrodes by using vacuum deposition technology.[14–19] Another high contrast solution involves making black matrices of the pixels through lithography process technology to reduce visual reflective sensitivity.[20,21] However, black electrodes and/or black matrices do not belong to the original architecture of OLEDs. Thus, they lead to extra fabrication complexity and costs.

In this study, we use a transfer matrix method with thin-film optical filters and the definition rule of color

Correspondence concerning this article should be addressed to H. S. Wu at cehswu@saturn.yzu.edu.tw.

performances in the 1931 index proposed by the Commission International de l'Eclairage (CIE_{1931}) to investigate the reflection and color saturation of the panel of an OLED. According to the theoretical ratiocinations, we chose an adaptable dye-polarizer composed of optical film to improve the visual sensitivity, color saturation, and CR. The theoretical simulation and experimental data are able to provide information of both academic and practical significance.

Theory and Rule

The theory of thin-film simulation

The multilayer thin-films of OLEDs are deposited on the substrate, including the transparent anode, the organic multilayers, and the metal cathode. The reflectance of the panel of an OLED can be described by the theory of thin-film simulation, which has a like transfer matrix of thin-film optical filters.[22] A high contrast OLED can also be fabricated by the theory of this method. The concept is based on using these materials with the gradient or graded refractive index to development a high contrast OLED.[13] The optical properties of any material are determined largely by the electrons and their interaction with electromagnetic disturbances. Refractive index is defined as the ratio of the velocity of light in free space c to the velocity of light in the medium v. When the refractive index is real, it is denoted by n. However, it is frequently complex, in which case it is denoted by N.

$$N = c/v = n - ik \tag{1}$$

N is often called the complex refractive index, n is called the real refractive index (or often simply refractive index), and k is the extinction coefficient. N is always a function of λ.

Light waves are electromagnetic, and a homogeneous, plane-polarized harmonic (or monochromatic) wave may be represented by the functions of electric field and magnetic field. There are fundamentally difficult ratiocinations and definitions associated with the expression of reflectance.

$$\delta = 2\pi N/d \tag{2}$$

$$R(\lambda) = [(y_0 - y_1)/(y_0 + y_1)][(y_0 - y_1)/(y_0 + y_1)]^* \tag{3}$$

where δ, d, y_0, and y_1 are phase indices. The wave allows for a shift in the z coordinate of the medium from 0 to d, as well as the admittance of the incident medium and the admittance of the substrate upon which the thin-film system is deposited. The reflectance of a thin film on the substrate is calculated through the concept of optical admittance.

$$y_1 = \boldsymbol{C}/\boldsymbol{B} \tag{4}$$

where

$$\begin{bmatrix} \boldsymbol{B} \\ \boldsymbol{C} \end{bmatrix} = \begin{bmatrix} \cos\delta & (i\sin\delta)/\eta \\ i\eta\sin\delta & \cos\delta \end{bmatrix} \begin{bmatrix} 1 \\ \eta_s \end{bmatrix} \tag{5}$$

η and η_s represent thin-film admittance and substrate admittance.

We replace the multilayer by a single surface which presents an admittance $\overline{Y}$, which is the ratio of the total tangential magnetic and electric fields and is given by

$$\overline{Y} = C/B \tag{6}$$

This result can be immediately extended to the general case of an assembly of $\boldsymbol{q}$ layers. The expression of reflectance is as follow

$$R(\lambda) = [(y_0 - \overline{Y})/(y_0 + \overline{Y})][(y_0 - \overline{Y})/(y_0 + \overline{Y})]^* \tag{7}$$

where

$$\begin{bmatrix} B \\ C \end{bmatrix} = \left\{ \prod_{r=1}^{q} \begin{bmatrix} \cos\delta_r & (i\sin\delta_r)/\eta_r \\ i\eta_r\sin\delta_r & \cos\delta_r \end{bmatrix} \right\} \begin{bmatrix} 1 \\ \eta_s \end{bmatrix} \tag{8}$$

or

$$\begin{bmatrix} B \\ C \end{bmatrix} = [M_1][M_2]\cdots[M_q] \begin{bmatrix} 1 \\ \eta_s \end{bmatrix} \tag{9}$$

M_1 indicates the matrix associated with layer 1, and so on.

The definition of the rule of color performances in CIE_{1931}

No existing display technology can produce the entire range of colors. The range of color a display device can produce is called the color gamut. It is commonly represented as the areas on the chromaticity diagram. For any three real primaries, it is sometimes necessary to supply a negative amount to reach some colors. That is, it is simpler to deal with a color space whose tristimulus values are always positive. Thus, the CIE has defined alternative color-matching functions such that any color may be matched with positive primary coefficients. These color-matching functions are called $\bar{x}(\lambda)$, $\bar{y}(\lambda)$, and $\bar{z}(\lambda)$. These functions are the result of experiments in which the stimulus spans 2° of the visual angle. Therefore, these are known as the color performances in the CIE_{1931}. A spectral stimulus may now be matched in terms of these color-matching functions, as follows[23,24]

$$Q_\lambda = \bar{x}(\lambda)X + \bar{y}(\lambda)Y + \bar{z}(\lambda)Z \tag{10}$$

For a given stimulus Q_λ, the tristimulus values (X, Y, Z) are obtained by integration, as follows

$$X = \int_{400}^{700} Q_\lambda \bar{x}(\lambda)d\lambda \tag{11}$$

$$Y = \int_{400}^{700} Q_\lambda \bar{y}(\lambda)d\lambda \tag{12}$$

$$Z = \int_{400}^{700} Q_\lambda \bar{z}(\lambda)d\lambda \tag{13}$$

The CIE XYZ matching functions are defined such that a theoretical equal-energy stimulus, which would have unit radiant power at all wavelengths, maps the tristimulus value (1, 1, 1). Further, note that $\bar{y}(\lambda)$ is equal to $V(\lambda)$ (CIE photonic luminous efficiency curve or visual factor)—another intentional choice by the CIE. Thus, Y represents photometrically weighted quantities. Associated tristimulus values are chromaticity coordinates, which may be computed from tristimulus values as follows.

$$x = \frac{X}{X + Y + Z} \tag{14}$$

$$y = \frac{Y}{X + Y + Z} \tag{15}$$

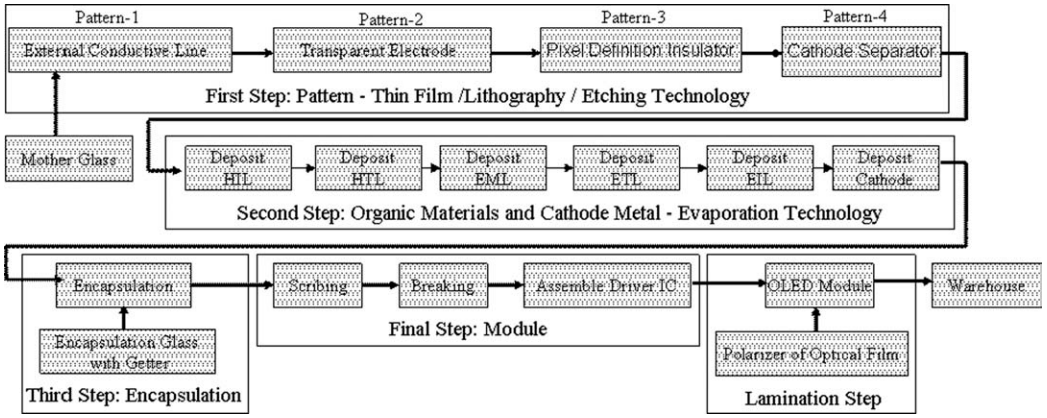

Figure 1. The process flow of panel in the PMOLED

$$z = \frac{Z}{X+Y+Z} = 1 - x - y \tag{16}$$

z is known if x and y are known. Thus, only the chromaticity coordinates of the latter two needs to be kept. Chromaticity coordinates are relative, which means that within a given system of primary stimuli, two colors with relative spectral power distribution will map to the same chromaticity coordinates.

The definition of CR

It is generally considered that the most important visual characteristic of a display is the CR of a visual image. The CR refers to the difference in visual properties that makes an object distinguishable from other objects and the background. Moreover, the CR indicates the gap between maximum brightness and maximum darkness. It conveys information by modifying an array of dots on a screen in the sole function of a display. The CR indicates the amount of difference that can be used to discriminate between a pixel that is fully on and on that is off in the reflection of ambient light. Furthermore, the CR is a key vision index of a display and is defined as[19,25,26]

$$\mathrm{CR} = \frac{(L_{\mathrm{on}} + R \times L_{\mathrm{amb}})}{(L_{\mathrm{off}} + R \times L_{\mathrm{amb}})} \tag{17}$$

In which CR, R, L_{on}, L_{off}, and L_{amb} represent CR, the reflectance of the panel, the luminance of the OLED when turned on, the luminance of the OLED when turned off, and the luminance of ambiance light, respectively.

Experimental Studies

Experimental OLED manufacturing

In this experiment, the panel of the bottom emission of a passive-matrix OLED (PMOLED) was made. The process flow of the panel of the experimental OLED followed the mass production procedure, as shown in Figure 1.[20,27]

According to the representation of Figure 1, a 0.7-mm-thick mother glass substrate was used, and an ITO film with a thickness of 150 nm was deposited on the surface of the mother glass, which had the optimal electricity and optic properties.[19] The average electro-optical property of the ITO substrate provides transmittance greater than 85% in the visible region and less than 10 Ω/□ sheet resistances. The first step of the process flow included the patterns of the four layers in the thin film, lithography, and the etching processes of the ITO substrate. The procedures of the first step included the metal alloy pattern of the external conductive line (e.g., Ag), the pattern of the transparent electrode (e.g., ITO), the insulator pattern of the pixel definition, and the separator pattern of the cathode metal. In the second step, the multiorganic layers and cathode metal layer (e.g., aluminum) were made by using evaporator technology. Therefore, the material of HIL, which reduces the energy barrier in between ITO and hole transport layer (HTL), is beneficial to enhancing charge injection at the interfaces and ultimately improving power efficiency of the device, the materials of HIL are that starburst amorphous materials, 4,4′,4″-tris(3-methyl-phenyl-phenylamino)triphenylamine can be doped by 3% strong molecular acceptors tetrafluoro-tetracyano-quinodimethane in the controlled coevaporation.[28] The material of HTL has a "bi-phenyl" center core that is a *N*,*N*′-bis(1-naphthyl)-*N*,*N*′-diphenyl-1,1′-biphenyl-4,4′diamine. The materials of EML use the fluorescent dopants in the guest-host doped emitter system, the red emitting materials that are 2% 4-(dicyanomethylene)-2-tert-butyl-6(1,1,7,7-tetramethyljulolidin-4-yl-vinyl)-4H-pyran to be doped in 5,6,11,12-tetraphenyl-naphthacene (Rubrene) and tris(8-hydroxyquinolinato)aluminum (Alq_3) of a cohost system, the green emitting materials that are 6% GD-206 of Idemitsu Kosan to be doped in BH-120 of Idemitsu Kosan, and the blue emitting materials that are 2% BD-52 of Idemitsu Kosan to be doped in BH-120 of Idemitsu Kosan. The material of ETL is Alq_3. The material of EIL is lithium fluoride (LiF); an effective cathode Al for OLEDs could be constructed by interposing a thin LiF layer between Al and Alq_3.[29,30] These organic materials were purchased from Syntec GmbH (Wolfen, Germany), Aldrich (Missouri, MO), Eastman Kodak (Rochester, NY), Idemitsu Kosan (Moji/Japan), respectively. In consideration of production yield, the thicker thicknesses of organic material layers and cathode metal-Al layers were considered to avoid the defect issues caused by the spike of ITO, pin holes of films, and thermal stability of light-emitting and particles.[31–33] The HIL/HTL/EML(R/G/B)/ETL/EIL thicknesses in the organic materials and cathod metal-Al were controlled to be 200/20/(R:20/G:18/B:25)/20/0.1 and 300 nm, respectively. In the third step, the mother glass substrate with patterns was encapsulated by an encapsulation mother glass substrate with getter to control the H_2O/oxygen-free

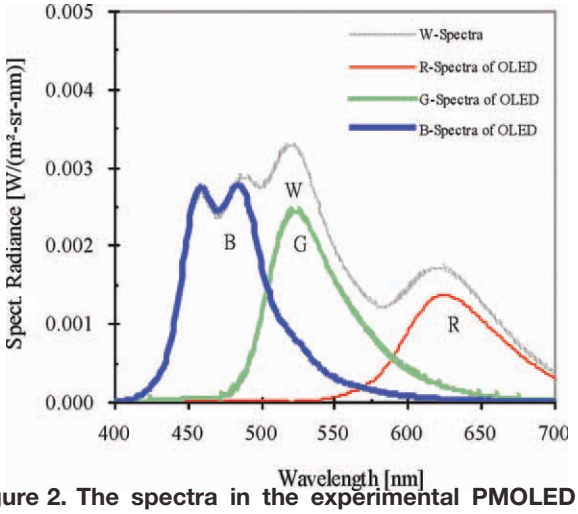

Figure 2. The spectra in the experimental PMOLED is turned on by driver IC at 13.5 V and measured by a Minolta Chroma Meter CS-1000 in a darkroom.

[Color figure can be viewed in the online issue, which is available at wiley onlinelibrary.com.]

environment. The final step involves module technology. In this step, the encapsulated substrate was scribed and broken according to the size of the design and assembled with the driver Integrated Circuit (IC), which is able to tune gamma curves in relation to grayscale and brightness.[34] The experimental PMOLED panel was formatted in the specification of 1.5″-128RGBx128 with 262,144 colors, and its basic spectra properties are shown in Figure 2. According to the spectra shown in Figure 2, the red coordinates (x,y) of CIE_{1931} are (0.630,0.354), the green coordinates (x,y) of CIE_{1931} are (0.294,0.630), and the blue coordinates (x,y) of CIE_{1931} are (0.145,0.193). The color saturation, when compared with the standard of the National Television System Committee (NTSC), is 59.4% and the synthetic white luminance is 145 (cd/m^2) when turning on red, green, and blue simultaneously.

The dye-polarizer property of an optical films

The optical films are deposited and laminated on the surface of a substrate to change the conveyors of wavelength, including the polarizer, phase compensator, brightness enhancement film, light collimated sheet, diffusion film, reflector, anti-reflection film, anti-glare film, and so on. The polarizer is an important component in the LCD field, because it can polarize the light from backlight source of an LCD. Conversion of a wave from linear to circular polarization may be effected by either transmission or reflection. When polarizers are manufactured, the polyiodine molecules are absorbed into a semicrystalline polymer film, and the film is drawn to have a high degree of orientation. The polyiodine molecules are also oriented in agreement with the polymer, and the film so obtained exhibits light absorption dependent on the polarization direction of incident light.[35,36] In free space with millimeter wavelengths, reflection circular polarizers are preferable to their less compact transmission counterparts.[37] Another function of polarizers is that they are able to protect the panel from scraping. Previous studies have discussed the optical properties of dye polarizers[38,39] and a new model has been developed to account for the dependence of optical anisotropy.[40] About the relative compositions of a dichroic dye in the applied dye-polarizer, they are like some polymer formulas with azo or polycyclic or anthraquinone compounds or mixtures and so on.[36,41,42] The applied dye-polarizers were purchased from Optimax (Taiwan). Dye-polarizers have better transparency in the red and blue regions of visible light and better temperature tolerance than typical iodide-polarizers. A dye-polarizer with a convenient, laminated display panel is considered here.

Measurement inspection

The electro-optical performance of the panel of the experimental PMOLED was verified and confirmed by the following instruments and measurement inspections. The color performances of the experimental PMOLED were measured in accordance with the CIE_{1931}. Color gamut (color saturation) and the current-luminance-voltage curve of the experimental PMOLED were measured by a Minolta Chroma Meter CS-1000. The panel of the experimental PMOLED was simulated in different light conditions, including indoor ambience, and outdoor ambience, by using a DMS-505 type autronic-Melchers GmbH. The transparent and reflecting performance of the dye-polarizer and the reflecting performance in the panel of the experimental PMOLED were measured by the Hitachi U4100 system.

Results and Discussion

Effects of the visual reflective sensitivity of human eyes

As mentioned above, the architecture of the organic layers of an OLED is a sandwich between the hole-injecting anode (ITO) and the electron-injecting cathode (Al) including a PMOLED and an active-matrix OLED. The optical property of multiorganic-layer thin films of an OLED can be described by the transfer matrix of thin-film optical filters. The cathode Al of the OLED has a strong reflection from the ambient light; the reflectance of the panel of an OLED can be simulated by thin-film simulation. This type of simulation is nonlinear for the visual sensitivity of human eyes and it is changed by wavelength. The green region (525–580 nm) is the best sensitivity region for human eyes for both daytime and nighttime light.[43,44] Using Eqs. 7 and 8 of thin-film simulation, the simulation of the reflectance in the panel of the experimental OLED is shown in Figure 3. Figure 3 shows that the reflective simulation of the panel of the experimental OLED including a high amount of green reflective wavelength region for the visual sensitivity of human eyes, and displayed a dye-polarizer composed of optical film with better transparency in the red and blue region and lower transparency in the green region in the visible light range. As shown in the results of Figure 3, the panel was ratiocinated, improving the visual reflective sensitivity of human eyes in the visible wavelength range when using a dye-polarizer on the panel of an OLED.

As mentioned above, we applied the optical transmittance property of a dye-polarizer to reduce the effect of reflective light on human eyes that is caused by ambient light, as shown in Figure 4. According to Figure 4, the dye-polarizer was obviously able to reduce the visual reflective sensitivity by 86.6% in the best sensitivity region of the human eyes on the panel of the experimental OLED.

According to the results of Figures 3 and 4, we obtained similar trend in the simulation and experimental

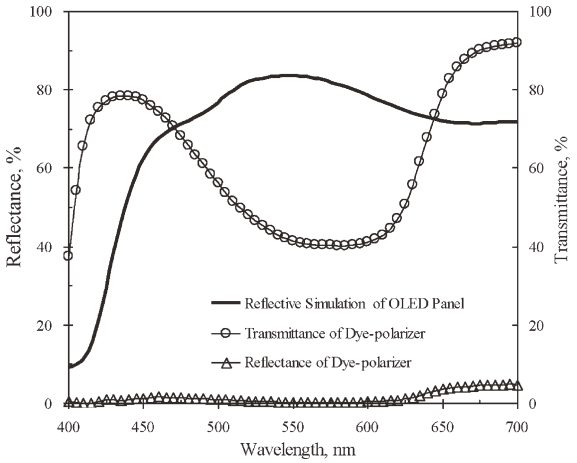

Figure 3. The simulation of the reflectance of the experimental OLED and the transmittance and reflectance of the dye-polarizer.

The reflectance was simulated by the thin-film simulation and the transmittance and reflectance were measured by the Hitachi U4100 system.

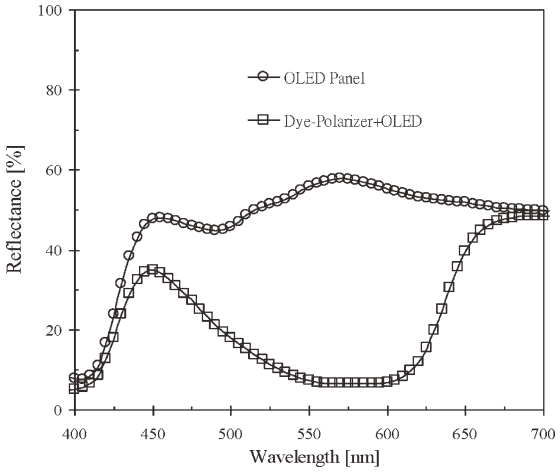

Figure 4. The reflectance of the panel of the experimental OLED and applying application of a dye-polarizer on the panel of the OLED panel.

The reflectance was measured by the Hitachi U4100 system.

measurement of the reflectance of the panel of the experimental OLED. Because the multiorganic layers between the hole injecting anode (ITO) and the electron injecting cathode (Al) were made by using evaporator technology, and the interfaces of them are not very perfect to cause the interference of a light. Therefore, the reflectance of the OLED panel obtained from simulation was higher than that obtained from experimental measurement.

Effects for the color coordinates of CIE_{1931} and color saturation

According to rules of color performances defined by CIE_{1931}, the red, green, and blue coordinates (x,y) of CIE_{1931} and color saturation are comparable with the standards of the NTSC. The CIE_{1931} index and color saturation are able to indicate the representations of hues. Larger hues or gamuts offer clearer discrimination for the vision of human eyes. They are also key vision indexes of displays.[45] According to Eqs. 10–14, we may obtain better a color saturation of red and blue for getting a smaller y value. This means that we can get a smaller numerator and/or a larger denominator in Eq. 15. When using a dye-polarizer on the panel of an OLED in the dark ambience, we can remodify the spectral stimulus on the panel of the experimental OLED. Equations 11–13 of the tristimulus values (X, Y, Z) are modified and obtained by integration, as follows.

$$X = \int_{400}^{700} (Q_\lambda \bar{x}(\lambda) \times T_{\text{dye-polarizer}}(\lambda))d\lambda \tag{18}$$

$$Y = \int_{400}^{700} (Q_\lambda \bar{y}(\lambda) \times T_{\text{dye-polarizer}}(\lambda))d\lambda \tag{19}$$

$$Z = \int_{400}^{700} (Q_\lambda \bar{z}(\lambda) \times T_{\text{dye-polarizer}}(\lambda))d\lambda \tag{20}$$

In which, $T(\lambda)_{\text{dye-polarizer}}$ is the transmittance of a dye-polarizer for optical films at different wavelengths, which leads them to Eqs. 14–16. The simulated and measured spectra of the panel of the experimental OLED with a dye-polarizer is shown in Figure 5. However, there was very thin glue exited between the experimental OLED panel and the using dye-polarizer in a practical lamination application. The glue is like an optical interference layer to obstruct the transmittance of a display. Therefore, the spectra of the OLED panel obtained from simulation were higher than that obtained from experimental measurement. According to the results in Figure 5, the proposed technique is able to modify the color saturation of the panel of the experimental OLED to achieve better color performance for visual effect.

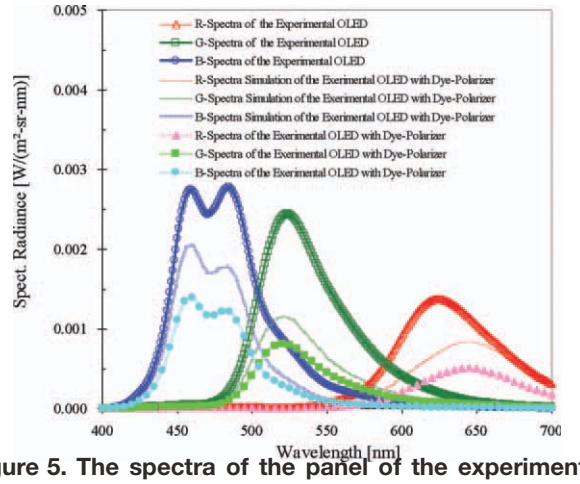

Figure 5. The spectra of the panel of the experimental OLED and its simulated and measured spectra with a dye-polarizer.

The spectra of the panel of the experimental OLED was measured by a Minolta Chroma Meter CS-1000 and the simulated spectra was modified by the modified equation of the definition rule of the color performances defined in the CIE_{1931}. [Color figure can be viewed in the online issue, which is available at wileyonlinelibrary.com.]

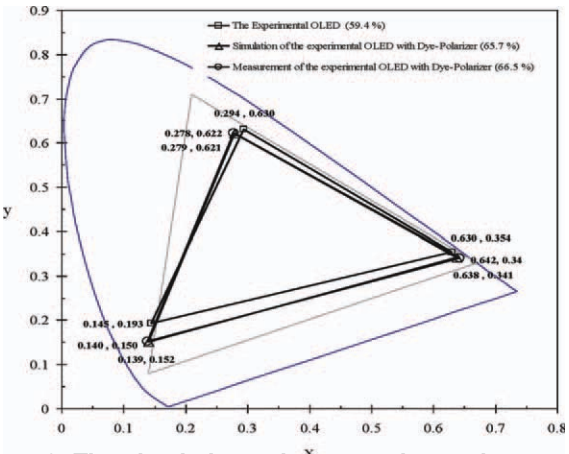

Figure 6. The simulation color saturation and measurement color saturation of the panel of the experimental OLED with and without a dye-polarizer.

The color saturation of the panel of the experimental OLED was measured by a Minolta Chroma Meter CS-1000 and the simulated color saturation was modified by a modified equation of definition rule of the color performances defined in the CIE_{1931}.

The improved color saturation results of the panel in the experimental OLED are shown in Figure 6. As seen in Figure 6, the color saturation of the panel of the experimental OLED with and without the dye-polarizer were measured by a Minolta Chroma Meter CS-1000. According to the results of Figure 6, the simulation and instrumental measurement of the panel of the experimental OLED with a dye-polarizer were very similar (65.7 and 66.5%), and the proposed technique was able to achieve better color performance, increasing the color saturation from 59.4 to 66.5% in the instrumental measurement.

According to the information provided by organic fluorescent materials,[44,46–50] the lifetime and efficiency of blue and red organic fluorescent materials are weaker than those of light blue and orange materials. With similar ratiocination, the CIE_{1931} index and color saturation of the OLED with a dye-polarizer and light blue and orange organic fluorescent materials instead of blue and red fluorescent materials are listed in Table 1. According to Table 1, we obtained similar color saturation for another experimental OLED with a dye-polarizer using light blue and orange organic fluorescent materials (increasing from 51.4 to 59.7%) in comparison to the color saturation (59.4%) of the original experimental OLED with blue and red organic fluorescent materials. The purpose of the combination of a dye-polarizer with light blue and orange organic fluorescent materials was to improve device characteristics such as lifetime, efficiency, and color saturation. Although organic phosphorescent materials are able to improve the lifetime and efficiency of the blue and red devices of OLEDs, however, they are more expensive in price and have more complex organic sandwich architectures than organic fluorescent materials.[51–53]

Effects of CR and color saturation in the different ambient lights

According to the visual reflective sensitivity of human eyes, we attempted to conduct a discussion of the CR of a display in an indoor ambience and an in outdoor ambience. It is generally considered that the most important visual characteristic of a display is the CR of an image. Conveying information by modifying an array of dots on a screen is the sole function of a display. The CR indicates the amount of difference that can be used to discriminate between a pixel that is fully on and one that is off in the reflection of ambient light. The CR is presented in Eq. 17. The ambient lights were simulated by the DMS-505 system of the autronic Melchers GmbH. The simulation included simulated indoor ambient light (490 cd/m^2) and simulated outdoor ambient light (1375 cd/m^2). These simulated spectra are shown in Figure 7. According to the spectra in Figure 7, the panel of the OLED was able to investigate the CRs under the conditions of simulated indoor ambience and simulated outdoor ambience.

According to the calculation of Eq. 17, better a CR value was obtained when using a dye-polarizer on the panel of the experimental OLED with different simulated ambient lights. These results are listed in Table 2. As shown in Table 2, the dye-polarizer was able to increase the CR of the panel by 2.4–2.7 times in a simulated indoor ambience (490 cd/m^2) and a simulated outdoor ambience (1375 cd/m^2).

We also conduct a discussion of color saturation for the color sensitivity of human eyes in different simulated ambient lights. The color saturations of the panel of the experimental OLED in different simulated ambient lights are shown in Figure 8a. According to Figure 8a, the color saturations of the panel of the experimental OLED obviously decreased from 59.4 to 30.9% in simulated indoor ambient light and from 59.4 to 17.9% in simulated outdoor ambient light.

According to Eqs. 18–20, the tristimulus values (X, Y, Z) are modified by using a dye-polarizer on the panel of the OLED in the dark ambience. For the panel of an OLED in the ambient light, the reflective factor is considered. Using a dye-polarizer on the panel of the OLED improved the color saturation of the panel of the experimental OLED in

Table 1. The Color Saturation of the Experimental OLED

CIE_{1931}		OLED with Blue and Red Organic Fluorescent Materials Without Dye-Polarizer	OLED with Light Blue and Orange Organic Fluorescent Materials	
			Without Dye-Polarizer	With Dye-Polarizer
Red	x	0.630	0.626	0.626
	y	0.354	0.364	0.359
Green	x	0.294	0.311	0.286
	y	0.630	0.633	0.634
Blue	x	0.145	0.151	0.142
	y	0.193	0.250	0.195
NTSC (%)		59.4	51.7	59.7

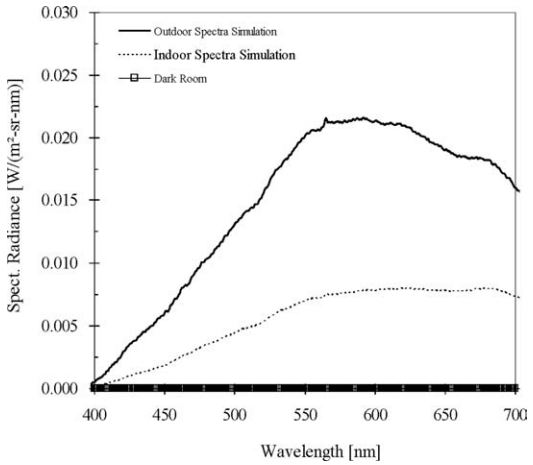

Figure 7. The spectra of indoor ambience and outdoor ambience were simulated by the DMS-505 system of the autronic Melchers GmbH.

simulated ambient lights. The ratiocination equation of color saturation in ambient light was modified by Eqs. 18–20. Because the second reflective factor is being small, we can neglect it. Equations 21–23 were modified and obtained by integration, as follows

$$X = \int_{400}^{700} (Q_{\lambda}\bar{x}(\lambda) \times T_{\text{dye-polarizer}}(\lambda) + L(\lambda) \times R_{\text{dye-polarizer}}(\lambda))d\lambda \tag{21}$$

$$Y = \int_{400}^{700} (Q_{\lambda}\bar{y}(\lambda) \times T_{\text{dye-polarizer}}(\lambda) + L(\lambda) \times R_{\text{dye-polarizer}}(\lambda))d\lambda \tag{22}$$

$$Z = \int_{400}^{700} (Q_{\lambda}\bar{z}(\lambda) \times T_{\text{dye-polarizer}}(\lambda) + L(\lambda) \times R_{\text{dye-polarizer}}(\lambda))d\lambda \tag{23}$$

In which, $L(\lambda)$ and $R(\lambda)_{\text{dye-polarizer}}$ are the strength of ambient light and the reflectance of the dye-polarizer composed of optical film at different wavelengths, which lead them to Eqs. 14–16. The simulation and instrumental measurement of the color saturation of the panel of the experimental OLED are shown in Figures 8b, c.

According to the results of Figures 8b, c, we obtained similar values in the simulation and instrumental measurement of the color saturation of the panel of the experimental OLED. According to the results of Figure 8a, c, it was able to retard color chromatism decay from 48 to 25.4% in simulated indoor ambient light and from 69.9 to 45.8% in simulated outdoor ambient light when using a dye-polarizer on the panel of the experimental OLED.

Table 2. Comparison of CR Value with and without Utilizing a Dye-Polarizer on the Panel of the OLED

Simulating Ambiance	Without Dye-Polarizer	With Dye-Polarizer
Indoor (490 cd/m^2)	1	2.7
Outdoor (1375 cd/m^2)	1	2.4

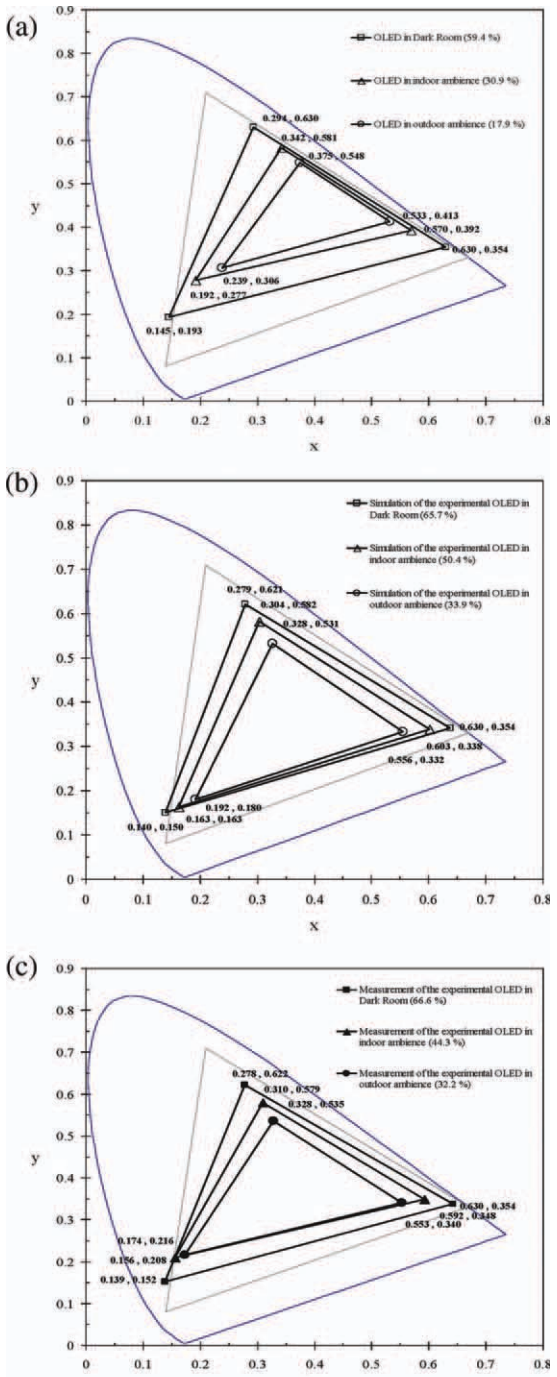

Figure 8. (a) The color saturation of the experimental OLED in a simulated indoor ambience (490 cd/m^2) and a simulated outdoor ambience (1375 cd/m^2).

(b) The simulation of the color saturation of the experimental OLED with a dye-polarizer in a simulated indoor ambience (490 cd/m^2) and a simulated outdoor ambience (1375 cd/m^2). (c) The measurement of the color saturation of the experimental OLED with a dye-polarizer in a simulated indoor ambience (490 cd/m^2) and a simulated outdoor ambience (1375 cd/m^2).

According to the optical interface theory, depositing multilayers like black electrodes or making black matrixes has the potential to improve the CRs of displays. However, these types of multilayers lead to extra costs and fabrication

complexity, which make it difficult to control product uniformity, maintain production throughput, and increase the product yield in the productions of OLEDs.[14–19] When depositing black cathodes or making black matrices of OLEDs, it is also necessary to laminate the protective film on the panel to avoid the scraping of OLEDs' panel surfaces.[20,21]

Light reflectance is expressed as a percentage and states how much of the light falling on a surface is reflected back. Generally, the reflect light of surface of a display will be caused by a strong ambient light. It will reduce the readability of human eyes and cause a decrease in the visible CR, color saturation of the screen image, and so on, for the visual reflective sensitivity of human eyes. Color saturation is used to describe the intensity of color in the image, which refers to how vivid and intense a color is. A display with poor color saturation will look washed out or faded. When the saturation level of color is reduced to 0, it becomes a shade of gray. However, larger color saturation offers cleaner discrimination for the vision of human eyes. For image performance, they are key vision indexes. The image performance can be resolve into these key elements, and it can also be expressed by the following mathematical function.

$$\text{Image performance} = f(\text{visual sensitivity},\ \text{contrast ratio},\ \text{color saturation},\ldots)$$

First, the panel of the OLED was ratiocinated by a transfer matrix of thin-film simulation and the rule of color performances defined in CIE_{1931} was used to investigate an adapted optical film. A dye-polarizer of composed optical film offers better transmittance of the red and blue regions applied on the panel of the experimental OLED. This obviously improves the visual performance of human eyes, including visual reflective sensitivity, color saturation, and CR in the ambient. It is easy and common to laminate a dye-polarizer on the panel of an OLED. This makes it unnecessary to develop a black cathode and/or black matrix. Black cathodes and/or black matrixes do not belong to the original OLED architecture. This lead to lots of difficulties and fabrication complexity (i.e., fabrication without damaging the underlying organic layers, the effects of absorbing and conducting, no additional barrier for electron injection, device compatibility, etc.) including extra costs.

Presently, the biggest obstacles in developing and marketing OLEDs are the expensive cost and immature supply chain, in comparison to LCDs. OLEDs costs almost seven times as much as LCDs'.[54] Currently, the most important step is to reduce the cost of OLEDs. Although depositing black cathodes and making black matrixes can improve the CR of images, these improvement actions lead to extra cost and fabrication complexity. Using dye-polarizers on the panels of OLEDs is a convenient and mature technique, which does not require the addition of extra technology. This method significantly improves the visual reflective sensitivity, CR, and color saturation under strong ambient light conditions.

Conclusion

In this study, the panel of an OLED has been successfully ratiocinated with the application of basic thin-film simulation and the rule of color performances in the CIE_{1931}. The proposed technique applied a dye-polarizer composed of optical film on the panel of an OLED. The proposed method was able to reduce the reflected light for visual reflective sensitivity of the human eye by 86.6% in ambient light and improve the CR by 2.4 times in simulated indoor ambiance (490 cd/m^2) and by 2.7 times in simulated outdoor ambiance (1375 cd/m^2). The proposed method was also able to improve the $CIE1_{931}$ value and color saturation from 59.4 to 65.7% in the theoretical simulation and 59.4 to 66.5% in the instrumental measurement. In a practical application, due to the weaknesses related to lifetime and the efficiency of red and blue organic fluorescent materials, this study used light blue and orange organic fluorescent materials instead. These ratiocination models were applied to investigate the visual performance of a display to choose the combination of an adapted optical film and the panel of an OLED.

Acknowledgments

The authors thank Professor Shaw S. Wang for instructing the writing of this journal article.

Literature Cited

1. Kalinowski J. *Organic Light-Emitting Diodes: Principle, Characteristics and Processes*. New York: Marcel Dekker, 2005
2. Li Z, Meng H. *Organic Light-Emitting Materials and Devices*. New York: Taylor & Francis, 2007.
3. Bhowmik AKB, Li Z, Bos PJ. *Mobile Displays*. Chichester, England: John Wiley & Sons, 2008.
4. Geffroy B, Roy P, Philippe PC, Christophe P. Organic light-emitting diode (OLED) technology: material, devices and display technologies. *Polym Int*. 2006;55:572–582.
5. Kido J, Hongawa K, Okuyama K, Nagai K. White light-emitting organic electroluminescent devices using the poly(*N*-vinylcarbazole) emitter layer doped with three fluorescent dyes. *Appl Phy Lett*. 1994;64:815–817.
6. Reineke S, Lindnerl F, Schwartzl G, Seiderl N, Walzerl K, Lusem B, Leo K. White organic light-emitting diodes with fluorescent tube efficiency. *Nature*. 2009;459:234–238.
7. Tang CW, VanSlyke SA. Organic electroluminescent diodes. *Appl Phys Lett*. 1987;51:913–915.
8. Tang CW, VanSlyke SA, Chen CH. Electroluminescent of doped organic thin films. *J Appl Phys*. 1989;65:3610–3616.
9. Young RH, Tang CW, Marchetti AP. Current-induced fluorescent quenching in organic light-emitting diodes. *Appl Phys Lett*. 2002;80:874–876.
10. Liu TH, Iou CY, Chen CH. Doped red organic electroluminescent devices based on a cohost emitter system. *Appl Phys Lett*. 2003;83:5241–5243.
11. Lu MH, Sturm JC. Optimization of external coupling and light emission in organic light-emitting devices: modeling and experiment. *J Appl Phys*. 2002;91:595–604.
12. Chen ML, Wei AC, Shieh HP. Increased organic light-emitting diode panel light efficiency by optimizing structure and improving alignment of pyramidal array light-enhancing layers. *Jpn J Appl Phys*. 2007;46:1521–1525.
13. Zhu F, Soo OK, Wei TL, Xiaotao H, Kwan LP. High contrast OLED. Sydney, NSW: *LEOS,* The 18th Annual Meeting of the IEEE. 2005;589–590.
14. Hung LS, Madathil JK. Reduction of ambient-light-reflection in organic light emitting devices. US Patent 6,429,451 B1, 2002.
15. Chen PY, Yokoyama M, Ueng HY. Increasing the contrast ratio of organic emitting diode by organic-metal light-absorbing layer in black cathode. *Jpn J Appl Phys*. 2010;49:12102-1–12102-4.
16. Huang ZH, Su WM, Zeng XT. Application of C60 for black cathode in organic light emitting diode. *SIMTech Tech Rep*. 2007;8:182–185
17. Kim OH, Ahn TJ. Organic electroluminescent device. US Patent 7,071,613 B2, 2006.
18. Hwang SH, Seo MK, Kang JH, Yang JY, Kang SY. A black metal-dielectric thin film for high-contrast displays. *J Korean Phys Soc*. 2009;55:501–507.
19. Hofstra PG, Krason AN. Organic electroluminescent device. US Patent 6,411,019 B1, 2002.

20. Lan WJ, Chang Chien CC. Organic light-emitting displays and their manufacturing. Taiwan Patent I 228,382, 2005.
21. Lee BD, Cho YH, Oh MH, Lee SY. Characteristics of contrast of active-matrix organic light-emitting diodes containing a block matrix and antireflection layers. *Mater Chem Phys*. 2008;112:734–737.
22. Macleod HA. *Thin-Film Optical Filters*. Philadelphia: Institute of Physics Publishing, 2001.
23. Reinhard E, Ward G, Pattanaik S, Debevec P. *High Dynamic Rang Imaging: Acquisyion, Display, and Image-Based Lighting*. New York: Morgan Kaufmann, 2006.
24. Koschan A, Abidi M. *Digital Color Image Processing*. New Jersey: John Wiley & Sons, 2008.
25. Xie WF, Zhao Y, Li CN, Liu SY. Contrast and efficiency enhancement in organic light-emitting device utilizing high absorption and high charge mobility organic layers. *Opt Exp*. 2006;14:7954–7959.
26. Xie WF, Sun HY, Law CW, Lee CS, Lee ST, Liu SY. High-contrast and high-efficiency top-emitting organic light-emitting device. *Appl Phys*. 2006;A85:95–97.
27. Nagayama K, Mjyaguchi S. Organic electroluescent display and method for manufacturing the same. US Patent 5,701,055, 1997.
28. Drechsel J, Pfeiffer M, Zhou X, Nollau A, Leo K. Organic mip-diodes by p-doping of amorphous wide-gap semiconductors: CV and impedance spectroscopy. *Synthetic Met*. 2002;127:201–205.
29. Hung LS, Tang CW, Mason MG. Enhanced electron injection in organic electroluminescence device using an Al/LiF. *Appl Phys Lett*. 1997;70:152–154.
30. Jabbour GE, Kawabe V, Shaheen SE, Wang JF, Morrell MM, Kippelen B, Peyghambarian N. High efficiency and bright organic electroluminescent device with an aluminum cathode. *Appl Phys Lett*. 1997;71:1762–1764.
31. Dos A, Paulo NM, Aziz H, Hu NX, Popovic ZD. Temperature dependence of electroluminescence degradation in organic light emitting devices without and with a copper phthalocyanine buffer layer. *Org Electron*. 2002;3:9–12.
32. Fujihira LMD, Koike A, Han EM. Growth of dark spots by interdiffusion across organic layers in organic electroluminescent devices. *Appl Phys Lett*. 1996;68:1787–1789.
33. McElvain J, Antoniads H, Hueschen MR, Miller JN, Roitman DM, Sheats JR, Moon RL. Formation and growth of black spots in organic light-emitting diodes. *J Appl Phys*. 2002;80:6002–6007.
34. Sempel A, Buchel M. Desifn Aspects of low power polymer/OLED passive-matrix displays. *Org Electron*. 2002;3:89–92.
35. Gunning WJ. Improvement in the transmission of iodide-polyvinyl alcohol polarizers. *J Appl Opt*. 1983;22:3229–3231
36. Matsuzaki Y, Oil R, Imai R, Takuma K, Itoh H. Azo compounds and polarizing films using the compounds. US Patent 5,698,682, 1997.
37. Jull EV. Reflection circular polarisers. *Electron Lett*. 1979;15:423–424.
38. Dirix Y, Tervoort TA, Bastiaansen C. Optical properties of oriented polymer/dye polarizer. *Marcomolecules*. 1995;28:486–491.
39. Dirix Y, Tervoort TA, Bastiaansen C. Optical properties of oriented polymer/dye polarizer. 2. Ultimate properties. *Marcomolecules*. 1997;30:2175–2177.
40. Han SE, Hwang IS. Modeling of the optical anisotropy of a dye. *J Polym Sci*. 2002;40:1363–1370.
41. Khan I, Bobrov GYA, Ignatov LY, Shishkina EY, Lazarev PI, Kurbatov AV. Dichroic light polarizers. US Patent 6,049,428, 2000.
42. Liu SH, Lin YC, Tzeng WS, Ma JH, Cheng KL, Lai LL. Dichroic dye, composition thereof, and liquid crystal display element containing the same. US Patent 6,861,106 B2, 2005.
43. Robinson MG, Chen J, Sharp GD. *Polarization Engineering for LCD Projection*. Chichester, England: John Wiley & Sons, 2008.
44. Chen CH, Huang SW. *OLED: Materials and Device of Dream Displays*. Taipei, Taiwan: Wunan, 2007.
45. Castellano JA. *Handbook of Display Technology*. New York: Academic Press, 1992.
46. Lee JH, Ho YH, Lin TC, Wu CF. High-efficiency fluorescent blue organic light-emitting device with blanced carrier transport. *J Elecron Soc*. 2007;154:J226–J228.
47. Huang Q, Walzer K, Feiffer MP, Lyssenko V, He G, Leo K. Highly efficient top emitting organic light-emitting diodes with organic outcoupling enchancement layers. *Appl Phys Lett*. 2006;88:113515–1135180.
48. Kohler A, Wilson JS, Friend RH. Fluorescence and phosphorescence in organic materials. *Adv Mat*. 2002;14:701–707.
49. Chew S, Wang P, Hong Z, Tao S, Tang J, Lee CS, Wong NB, Kwong H, Lee ST. High-performance organic red-light-emitting devices based on a greenish-yellow light-emitting host and long-wavelength emitting dopant. *Appl Phys Lett*. 2006;88:183504–1830506.
50. Hosokawa C, Fukuoka K, Kawamura H, Sakai T, Kubota M, Funahashi M, Moriwaki F, Ikeda H. Improvement of lifetime in organic electroluminescence. *SID Symp Dig Tech Papers*. 2004;35:780–783.
51. Baldo MA, O'Brien DF, You Y, Shoustikov A, Sibley S, Thompson ME, Forrest SR. Highly efficient phosphorescent emission from organic electroluminescent devices. *Nature*. 1998;395:151–154.
52. Baldo MA, Lamansky S, Burrows PE, Thompson ME, Forrest SR. Very high-efficiency green organic light-emitting devices based on electrophosphorescence. *Appl Phys Lett*. 1999;75:4–6.
53. Kohler A, Wilson JS, Friend RH. Fluorscence and phosphorescence in organic materials. *Adv Mat*. 2002;14:701–707.
54. Sengupta A. *Organic Material Lift Time: A Key to OLED Market Penetration?* Mountain View, CA: Frost & Sullivan, 2009.

Manuscript received Mar. 7, 2011, and revision received May 21, 2011.